

# Inhibition of p38 MAP kinase by utilizing a novel allosteric binding site

Christopher Pargellis<sup>1</sup>, Liang Tong<sup>2,3</sup>, Laurie Churchill<sup>1</sup>, Pier F. Cirillo<sup>2</sup>, Thomas Gilmore<sup>2</sup>, Anne G. Graham<sup>1</sup>, Peter M. Grob<sup>1</sup>, Eugene R. Hickey<sup>2</sup>, Neil Moss<sup>2</sup>, Susan Pav<sup>1</sup> and John Regan<sup>2</sup>

Departments of <sup>1</sup>Biology and <sup>2</sup>Medicinal Chemistry, Boehringer Ingelheim Pharmaceuticals, Research and Development Center, 900 Ridgebury Road, Ridgefield, Connecticut 06877, USA. <sup>3</sup>Department of Biological Sciences, Columbia University, New York, New York 10027, USA.

Published online: 18 March 2002, DOI: 10.1038/nsb770

**The p38 MAP kinase plays a crucial role in regulating the production of proinflammatory cytokines, such as tumor necrosis factor and interleukin-1. Blocking this kinase may offer an effective therapy for treating many inflammatory diseases. Here we report a new allosteric binding site for a diaryl urea class of highly potent and selective inhibitors against human p38 MAP kinase. The formation of this binding site requires a large conformational change not observed previously for any of the protein Ser/Thr kinases. This change is in the highly conserved Asp-Phe-Gly motif within the active site of the kinase. Solution studies demonstrate that this class of compounds has slow binding kinetics, consistent with the requirement for conformational change. Improving interactions in this allosteric pocket, as well as establishing binding interactions in the ATP pocket, enhanced the affinity of the inhibitors by 12,000-fold. One of the most potent compounds in this series, BIRB 796, has picomolar affinity for the kinase and low nanomolar inhibitory activity in cell culture.**

The proinflammatory cytokines tumor necrosis factor- $\alpha$  (TNF $\alpha$ ) and interleukin-1 $\beta$  (IL-1 $\beta$ ) mediate the inflammatory response associated with the immunological recognition of infectious agents. Elevated levels of proinflammatory cytokines are associated with several diseases of autoimmunity, such as toxic shock syndrome, rheumatoid arthritis, osteoarthritis, diabetes and inflammatory bowel disease<sup>1</sup>. An important and accepted therapeutic approach for potential drug intervention in these diseases is the reduction of proinflammatory cytokines. For example, clinical efficacy has been demonstrated with a solu-

ble TNF $\alpha$  receptor fusion protein, as well as a monoclonal antibody directed against TNF $\alpha$  for the treatment of rheumatoid arthritis<sup>2,3</sup>.

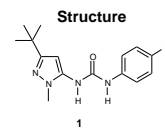
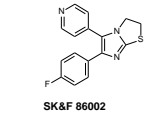
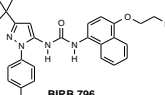
The p38 Ser/Thr MAP kinase plays a crucial role in the signal transduction cascade leading to the production of proinflammatory cytokines<sup>4</sup>. In our search for new inhibitors against this kinase, a high-throughput screen identified the diaryl urea compound **1** as a lead, with modest binding and cellular activities (Fig. 1). This compound bears little structural similarity to the pyridinyl-imidazole inhibitors<sup>5</sup> such as SB203580 (ref. 6) and, therefore, establishes a new class of inhibitors for p38 MAP kinase<sup>7</sup>.

## A new allosteric binding pocket

To define the binding mode of this new class of diaryl urea inhibitors and to establish the molecular mechanism for their inhibitory activity, we determined the crystal structure of human p38 MAP kinase in complex with compound **1** at 2.5 Å resolution (Fig. 2*a,b*; Table 1). The structure revealed that this compound utilizes a new allosteric binding pocket on the kinase that is spatially distinct from the ATP pocket (Figs 2*a*, 3*a*). The compound is oriented at ~60° to ATP. There is no structural overlap between the atoms of compound **1** and ATP. Similarly, there is only limited overlap between compound **1** and the pyridinyl-imidazole inhibitor<sup>8</sup> (Fig. 3*a*).

A large conformational change for residues in the conserved Asp-Phe-Gly (DFG) motif in the active site of the kinase is required for the binding of the inhibitor (Fig. 3*a*). In all of the known protein Ser/Thr kinase structures, the DFG motif assumes a conformation with the Phe residue buried in a hydrophobic pocket in the groove between the two lobes of the kinase (DFG-in conformation). The residues in this pocket are highly conserved among the kinases. In the structure of the complex with compound **1**, however, the Phe side chain has moved by ~10 Å to a new position (DFG-out conformation). In this position, one face of the Phe side chain helps to shield the inhibitor whereas the other face is exposed to solvent. This movement of the Phe side chain reveals a large hydrophobic pocket in the kinase, and the *t*-butyl group of compound **1** is inserted deep into this pocket (Fig. 3*b*). Structure-activity relationship (SAR) studies showed that replacing the *t*-butyl group with a methyl group produced a >1,000-fold reduction in activity, providing strong evidence for the importance of hydrophobic interactions in this new binding pocket. Neither nitrogen atom on the pyrazole ring is involved in specific hydrogen-bonding interactions with the kinase. Therefore, the pyrazole ring seems to be purely a scaffold for the correct positioning of both the *t*-butyl group and the urea pharmacophore.

The structural information suggests that the diaryl urea inhibitors have a new mechanism of inhibiting the p38 MAP kinase — indirectly competing with the binding of ATP. Most other protein kinase inhibitors use the ATP-binding pocket and inhibit the kinase by directly competing with ATP binding<sup>9,10</sup>. In contrast, compound **1** has no structural overlap with the ATP molecule (Fig. 3*a*). However, our structure shows that the DFG-out conformation is incompatible with ATP binding because the side chain of the Phe residue is in steric overlap with the phosphate groups of ATP (Fig. 3*a*). The indirect competition with

Structure	$k_{on}(M^{-1}s^{-1})$	$k_{off}(s^{-1})$	$K_d$ (nM)	Inhibition of TNF $\alpha$ in THP.1 IC <sub>50</sub> (nM)
	$1.2 \times 10^5$ $\pm 3.5 \times 10^4$	$1.4 \times 10^{-1}$ $\pm 1.2 \times 10^{-2}$	1,160	5,900 $\pm 400$
	$4.3 \times 10^7$ $\pm 2.2 \times 10^5$	7.7 $\pm 1.3 \times 10^{-1}$	180	3,500 $\pm 900$
	$8.5 \times 10^4$ $\pm 2.6 \times 10^2$	$8.3 \times 10^{-6}$ $\pm 1.5 \times 10^{-7}$	0.1	18 $\pm 3$

**Fig. 1** *In vitro* and *in vivo* data for selected p38 inhibitors.  $K_d$  was determined at 23 °C and calculated as  $k_{off} / k_{on}$  in nM.

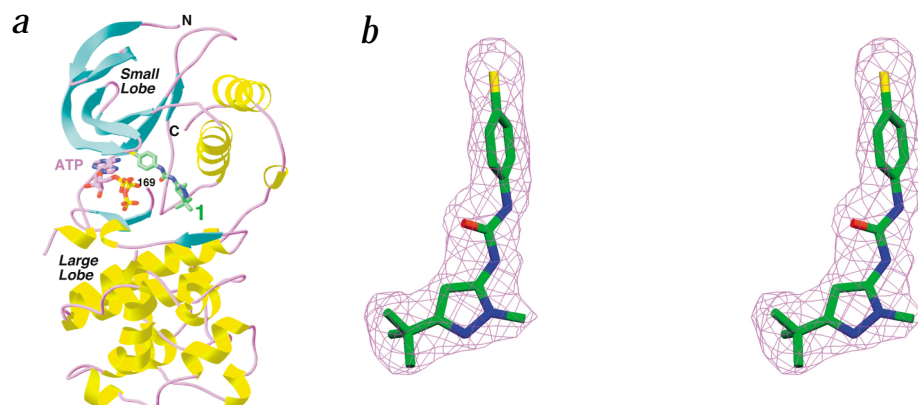


**Fig. 2** A new allosteric binding pocket for compound **1** in human p38 MAP kinase. **a**, Schematic drawing of the structure of p38 MAP kinase in complex with compound **1**. The inhibitor is shown as a stick model, with carbon atoms in green. The expected location of the ATP molecule<sup>8</sup> (purple for carbon atoms) is shown for reference. **b**, Final  $2F_o - F_c$  electron density map for compound **1**, contoured at  $1 \sigma$  level. Panel (a) is produced with RIBBONS<sup>27</sup> and panel (b) with SETOR<sup>28</sup>.

ATP binding is supported by our observation that compound **1** interferes with the inactivation of p38 MAP kinase by the fluorescent ATP analog 5'-*p*-fluorosulfonyl benzoyl adenosine (data not shown). Therefore, the diaryl urea compounds inhibit p38 MAP kinase by stabilizing a conformation of the kinase that is incompatible with ATP binding.

#### BIRB 796, a picomolar inhibitor of human p38 MAP kinase

Subsequent chemical synthetic efforts lead to the discovery of BIRB 796, a picomolar inhibitor of human p38 MAP kinase, with a 12,000-fold increase in binding affinity compared to compound **1** (Fig. 1). Three major structural changes were made to compound **1** that confer the observed increase in binding affinity: replacement of the methyl substituent on the pyrazole ring with a tolyl group (~140-fold enhancement in affinity), replacement of the chlorophenyl group with the naphthyl moiety (~15-fold) and the introduction of an ethoxymorpholine substituent on the naphthyl ring (~11-fold).

To understand the molecular basis for the enhanced affinity of these compounds, we determined the crystal structure of the kinase in complex with BIRB 796 at 2.8 Å resolution (Fig. 3c; Table 1). As with compound **1**, the kinase exists in the DFG-out conformation. The tolyl substituent on the pyrazole ring has favorable interactions with the hydrophobic portion of the side chain of the conserved Glu 71 residue in helix  $\alpha$ C (Fig. 3c). This tolyl group also caused a conformational change in the Glu 71 side chain. In the structure of the kinase in complex with compound **1**, the Glu 71 side chain carboxylate makes hydrogen bonds with both urea NH groups (Fig. 3c). In the complex with BIRB 796, the Glu 71 side chain can hydrogen bond to only one of the urea NH groups (Fig. 3c), but the new conformation of this side chain is best suited for hydrophobic interactions with the tolyl group of the inhibitor.

The structure reveals that the affinity enhancement by the morpholino substituent is probably due to a hydrogen bond with the main chain amide of residue 109 (Fig. 3c). This hydrogen bond, equivalent to the one made by the N1 atom of the adenine base of ATP, is crucial for the potency of the pyridinyl-imidazole inhibitors<sup>8</sup>, as well as most other protein kinase inhibitors. In addition to establishing interactions in the ATP pocket, the morpholino group also improves the physico-chemical properties of the inhibitor.

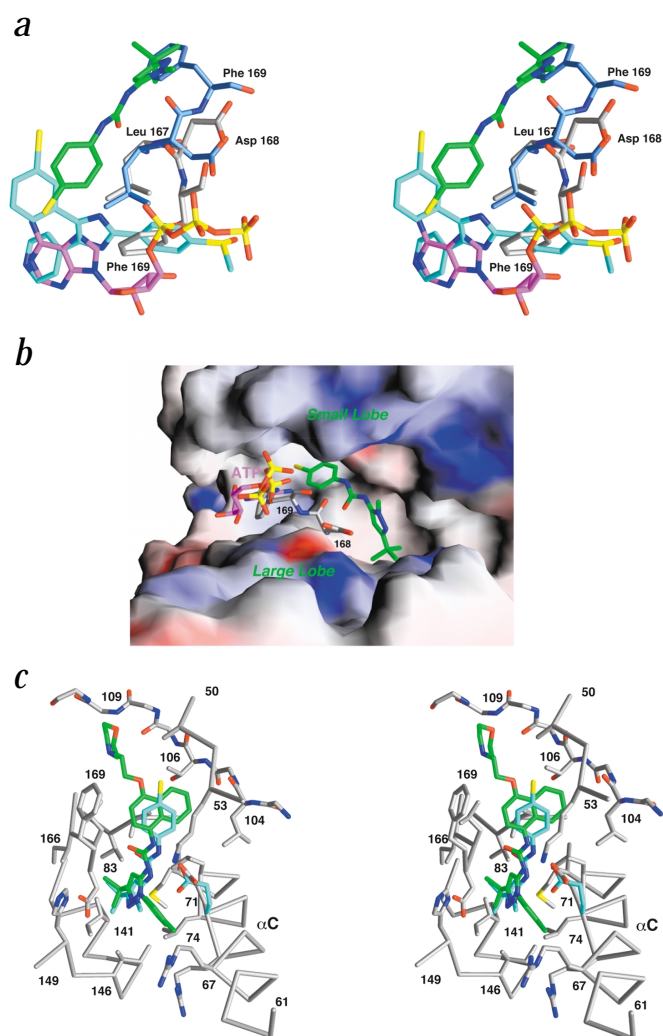


**Fig. 3** A conformational change in the kinase is required for the binding of diaryl urea inhibitors. **a**, Stereo view showing the conformational change for the DFG motif. The DFG-in conformation is shown with the carbon atoms in light blue, and the DFG-out conformation is in gray. Also shown is the overlay of the binding modes of compound **1** (green), the 3'-iodo analog of SB 203580 (cyan)<sup>8</sup> and ATP (purple). **b**, Molecular surface of the p38 MAP kinase in the active site region in complex with compound **1**. For clarity, residues in the DFG motif are shown as a stick model. The ATP molecule is shown for reference. **c**, Stereo view showing the binding pocket (gray for carbon atoms) for BIRB 796 (green). Also shown is compound **1** and the conformation of Glu 71 (cyan) in that complex. Produced with GRASP<sup>29</sup>.

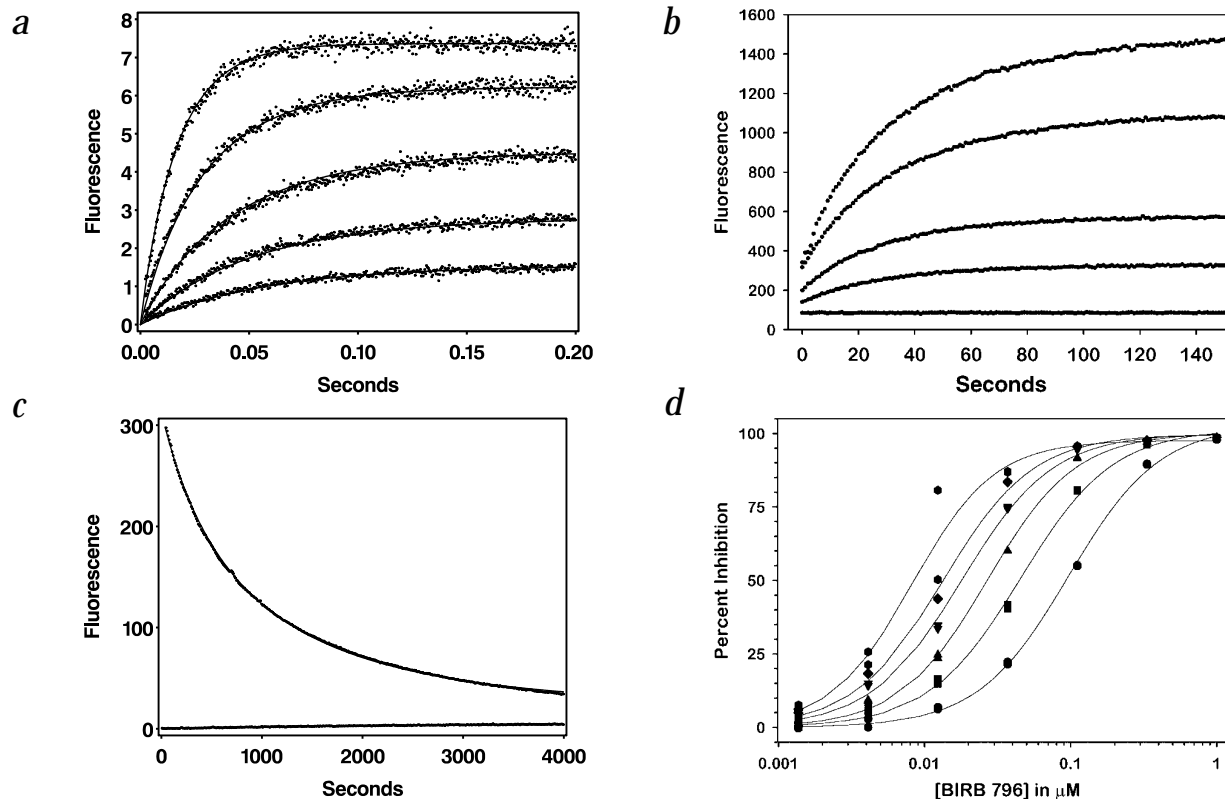


**Fig. 4** Kinetics of compound binding to p38 MAP kinase. **a**, Association curves for the binding of SK&F 86002 to p38 MAP kinase. The concentration of the kinase was 212 nM, and the concentrations of SK&F 86002 are (from top to bottom) 2,500 nM, 1,250 nM, 630 nM, 320 nM and 160 nM. **b**, Association curves for a fluorescent analog of BIRB 796. The concentration of p38 MAP kinase was 279 nM, and the concentrations of the fluorescent analog are (from top to bottom) 1,500 nM, 1,000 nM, 500 nM, 250 nM and 0 nM. **c**, Competitive binding between SK&F 86002 and BIRB 796. The concentration of p38 MAP kinase was 174 nM, and the concentration of BIRB 796 was 290 nM. **d**, Progression of apparent  $IC_{50}$  values of BIRB 796 for the following preincubation periods: filled circles, 0 min,  $IC_{50} = 97 \pm 4$  nM; filled squares, 15 min,  $IC_{50} = 45 \pm 3$  nM; filled upward triangles, 30 min,  $IC_{50} = 27 \pm 1$  nM; filled downward triangles, 60 min,  $IC_{50} = 18 \pm 1$  nM; filled diamonds, 90 min,  $IC_{50} = 13 \pm 1$  nM; and filled hexagons, 120 min,  $IC_{50} = 8 \pm 1$  nM.

### Time-dependent inhibition by diaryl urea compounds

To characterize the interactions of this new class of compounds with the kinase in solution, we established a fluorescence assay capable of monitoring binding in real time. The binding of the fluorophore SK&F 86002 (ref. 6) to nonactivated p38 MAP kinase was quite rapid, requiring the use of a stopped-flow spectrophotometer to determine kinetic rate constants<sup>11</sup> (Fig. 4a). Similarly, our results suggest that the compound SB203580 also has fast association and dissociation rates for the kinase. In contrast, the association of a fluorescent analog of BIRB 796 to p38 MAP kinase is much slower (Fig. 4b). Rate constants for the binding of nonfluorescent compounds were determined from competition assays with SK&F 86002 as the fluorophore<sup>12</sup> (Fig. 4c). The association rate constant for BIRB 796 is  $\sim 500\times$  slower than that of SK&F 86002, establishing BIRB 796 as a slow-binding inhibitor (Fig. 1). We also obtained similar kinetic results for the binding of either SK&F 86002 or BIRB 796 to pre-activated p38 (data not shown).

Notably, the dissociation rate constant for BIRB 796 is  $\sim 1,000,000\times$  slower than that for SK&F 86002. The improvement in the overall binding affinity from compound 1 to BIRB 796 is due almost exclusively to a reduction in the dissociation rate constant (Fig. 1). The calculated half-life for the dissociation of BIRB 796 from p38 MAP kinase is 23 h. This may have potential impact on *in vivo* efficacy, because slower dissociation may translate into extended dosing protocols<sup>13</sup>. BIRB 796 represents

one of the most potent and slowest dissociating inhibitors against human p38 MAP kinase now known.

To obtain further confirmation for the slow binding behavior, we monitored the apparent inhibitory potency of BIRB 796 as a function of the preincubation time in a standard  $IC_{50}$  experiment. A decrease in the apparent  $IC_{50}$  value from 97 nM to 8 nM after 2 h of preincubation is consistent with the slow binding behavior (Fig. 4d). In contrast, the pyridinyl-imidazole inhibitors reached equilibrium within 30 min (data not shown). In summary, the fluorescent binding assays and the time-dependence of apparent inhibitory potency confirm the slow binding behavior of the diaryl urea inhibitors.

### Molecular mechanism for the slow binding

The conformational change required for the binding of the diaryl urea compounds to p38 MAP kinase may be the molecular basis for the time-dependent inhibition. Similar observations have been made for several different enzyme-inhibitor systems<sup>14</sup>. The structural information and the slow-binding behavior suggest that p38 MAP kinase exists mostly in the DFG-in conformation, whereas the DFG-out conformation is sampled only infrequently. To our knowledge, this is the first time that the DFG-out conformation has been observed in a protein Ser/Thr kinase. In contrast, the DFG-out conformation seems to be more stable in protein Tyr kinases. The inactive insulin receptor tyrosine kinase exists almost exclusively in the DFG-out confor-

Table 1 Summary of crystallographic information

Structure	Compound 1	BIRB 796
Maximum resolution (Å)	2.5	2.8
Number of observations	31,423	22,129
R <sub>merge</sub> (%) <sup>1</sup>	4.6	5.3
Resolution range (Å)	20–2.5	20–2.8
Number of reflections	12,621	8,139
Completeness (%)	94	87
R-factor / R <sub>free</sub> (%) <sup>2</sup>	22.1 / 28.4	22.8 / 31.8
R.m.s. deviation		
Bond lengths (Å)	0.007	0.012
Bond angles (°)	1.3	1.6

$$^1R_{\text{merge}} = \frac{\sum_i \sum_h |I_{hi} - \langle I_h \rangle|}{\sum_i \sum_h I_{hi}}$$

$$^2R\text{-factor} = \frac{\sum_h |F_{o,h} - F_{c,h}|}{\sum_h F_{o,h}}$$

mation<sup>15</sup>, which also interferes with the binding of ATP<sup>16</sup>. Recently, the Abl tyrosine kinase in complex with the Novartis inhibitor, STI-571, was observed in the DFG-out conformation<sup>17</sup>. The binding mode of the STI inhibitor bears resemblance to the diaryl urea compounds described here. However, the Phe pocket is not fully occupied by the STI inhibitor. Moreover, the *t*-butyl group in our diaryl urea compounds has no equivalent in the STI inhibitor. Our structural and solution studies suggest that the conformational variability of the DFG motif may be a general phenomenon in the protein Ser/Thr and Tyr kinases that can be utilized in the design and development of new selective inhibitors against protein kinases.

### The diaryl urea inhibitors are highly selective

Selectivity is critical to the inhibition of protein kinases as a means of therapeutic intervention. Protein kinases are a large class of enzymes encoded by the human genome, and the degree of homology across the entire family is relatively high, especially within the catalytic core<sup>18</sup>. Nonetheless, the selectivity of BIRB 796 for the inhibition of p38 MAP kinase is high. No significant inhibition of the following 11 protein kinases is observed for BIRB 796: ERK-1, SYK, IKK2 $\beta$ , ZAP-70, EGF receptor kinase, HER2, protein kinase A (PKA), PKC, PKC- $\alpha$ , PKC- $\beta$  (I and II) and PKC- $\gamma$ . Three kinases show weak inhibition but with >1,000-fold selectivity over the inhibition of p38 MAP kinase: c-RAF-1 (IC<sub>50</sub> = 1.4  $\mu$ M), p59fyn (24  $\mu$ M) and p56lck (35  $\mu$ M). The inhibition of JNK2 $\alpha$ 2 by BIRB 796 (IC<sub>50</sub> = 0.098  $\mu$ M) still provides 330-fold selectivity. The inhibition of these latter four kinases does not seem to be time dependent.

The structural information also reveals the molecular mechanism for the high degree of selectivity of the diaryl urea inhibitors towards p38 MAP kinase. The structural overlap between these compounds and the pyridinyl-imidazole inhibitors is limited to the naphthyl substituent on the urea moiety and the 4-phenyl group on the imidazole ring, respectively (Fig. 3a). Our previous structural studies on the pyridinyl-imidazole inhibitor showed that this 4-phenyl ring is the determinant for the specificity<sup>8</sup>. This ring protrudes from the overall envelope of the ATP molecule and is located in a binding pocket that seems to be unique for p38 MAP kinase, partly due to the presence of a small Thr 106 residue in this pocket (Fig. 3c). The structural overlap shows that the diaryl urea inhibitors also utilize this binding pocket, thus explaining the high degree of selectivity of these inhibitors.

Our synthetic program has produced compounds that are highly potent and selective inhibitors of p38 MAP kinase, as indicated by both molecular and cellular assays. BIRB 796 demonstrated efficacy in an endotoxin (LPS)-stimulated mouse model

of TNF $\alpha$  release and in a mouse model of established collagen-induced arthritis (data not shown). Results from human phase I clinical trials indicate that BIRB 796 is well tolerated and shows good pharmacokinetic and pharmacodynamic properties. BIRB 796 also displayed anti-inflammatory effects in a trial of human endotoxemia<sup>19</sup>. This compound is now being evaluated in phase II clinical trials, including rheumatoid arthritis.

### Methods

**Protein synthesis, purification and crystallization.** BIRB 796 was synthesized as described<sup>20</sup>. SB203580 was purchased from Calbiochem. Non-activated human p38 MAP kinase was purified as described<sup>21</sup>. The crystallization conditions are essentially the same as those used earlier with the pyridinyl-imidazole inhibitor<sup>8,21</sup>, with the inclusion of 2–5 mM of trifluoroacetic acid in the crystallization solution. X-ray diffraction data were collected at 100 K on a R-Axis imaging plate system mounted on a Rigaku generator. The diffraction images were processed with the R-Axis software. The crystals belong to space group P2<sub>1</sub>2<sub>1</sub>2<sub>1</sub> and are isomorphous to those in complex with the pyridinyl-imidazole inhibitor<sup>8</sup>. The structure refinement was carried out with CNS<sup>22</sup>. The atomic models were manually rebuilt against the 2F<sub>o</sub> – F<sub>c</sub> electron density map with O<sup>23</sup>. The refinement statistics are summarized in Table 1.

**Binding studies.** Binding studies were conducted in a buffer containing 20 mM Bis-Tris Propane, pH 7.0, 2 mM EDTA, 0.01% (w/v) NaN<sub>3</sub> and 0.15% (w/v) n-octylglucoside. Kinetic data for the association of SK&F 86002 to p38 MAP kinase was collected on a Kintech fluorescence detector system equipped with a stopped flow controller. The data were fit simultaneously to an appropriate equation describing kinetic binding for a simple one-step binding mechanism<sup>11</sup>. The data for the binding of the fluorescent analog of BIRB 796 was corrected for background fluorescence of unbound ligand. The exchange curve assays were run as two half-reactions using an SLM Aminco Bowman Series 2 Model SQ-340 fluorescence detector<sup>11</sup>. In the first half-reaction, p38 MAP kinase and SK&F 86002 are preincubated for 3 min. In the second half-reaction, p38 MAP kinase is preincubated with BIRB 796 for 60 min. A net dissociation of the fluoroprobe is observed for the first half-reaction, and a net association is observed for the second half-reaction. The raw data from both half reactions are fit simultaneously to an equation describing simple competitive inhibition<sup>11</sup>.

p38 $\alpha$  was preactivated by treatment with constitutively active recombinant MKK6 (prepared by mutagenizing the two activation residues, Ser 189 and Thr 193, to Glu residues)<sup>24</sup>. Activated p38 $\alpha$  was purified and used as a source of enzyme in a standard kinase activity assay<sup>25</sup> monitoring the incorporation of radioactive phosphate into recombinant human MAPK $\alpha$  k2. Cellular assays followed published procedures<sup>4,26</sup>. Briefly, human THP.1 cells were stimulated with 1  $\mu$ g ml<sup>-1</sup> LPS, in the presence or absence of compound, followed by the determination of released TNF $\alpha$  using a commercial ELISA kit (Biosource).

**Coordinates.** The atomic coordinates have been deposited in the Protein Data Bank (accession codes 1KV1 and 1KV2).

### Acknowledgments

We are indebted to the following people: J. Pelletier, A. Proto and M. Basso for assistance with biological assays; A. Swinamer, B. Klaus and M. Moriaki for the preparation of various analogs of BIRB 796; M. Morelock for statistical analysis; L. Rondano for graphics support; and R. Winquist and P. Farina for useful discussions. We acknowledge Glaxo SmithKline Pharmaceuticals for the generous gift of SK&F 86002.

### Competing interests statement

The authors declare that they have no competing financial interests. Correspondence should be addressed to C.P. email: cpargell@rdg.boehringer-ingenheim.com or L.T. email: tong@como.bio.columbia.edu

Received 9 November, 2001; accepted 24 January, 2002.

1. Feldmann, M., Brennan, F.M., & Maini, R.N. *Annu. Rev. Immunol.* **14**, 397–440 (1996).
2. Weinblatt, M.E. *et al. N. Engl. J. Med.* **340**, 253–259 (1999).
3. Jarvis, B. & Faulds, D. *Drugs* **57**, 945–966 (1999).
4. Prichett, W., Hand, A., Shields, J., & Dunnington, D. *J. Inflamm.* **45**, 97–105 (1995).
5. Lee, J.C. *et al. Nature* **372**, 739–746 (1994).
6. Lee, J.C. *et al. Ann. NY Acad. Sci.* **696**, 149–170 (1993).
7. Dumas, J. *et al. Bioorg. Med. Chem. Lett.* **10**, 2047–2050 (2000).
8. Tong, L. *et al. Nature Struct. Biol.* **4**, 311–316 (1997).
9. Frantz, B. *et al. Biochemistry* **37**, 13846–13853 (1998).
10. Young, P.R. *et al. J. Biol. Chem.* **272**, 12116–12121 (1997).
11. Morelock, M.M., Pargellis, C.A., Graham, E.T., Lamarre, D. & Jung, G. *J. Med. Chem.* **38**, 1751–1761 (1995).
12. Pargellis, C.A. *et al. Biochemistry* **33**, 12527–12534 (1994).
13. Kaplan, A.P. & Bartlett, P.A. *Biochemistry* **30**, 8165–8170 (1991).
14. Cha, S. *Biochem. Pharmacol.* **24**, 2177–2185 (1975).
15. Hubbard, S.R., Wei, L., Ellis, L., & Hendrickson, W.A. *Nature* **372**, 746–754 (1994).
16. Hubbard, S.R., Mohammadi, M., & Schlessinger, J. *J. Biol. Chem.* **273**, 11987–11990 (1998).
17. Schindler, T. *et al. Science* **289**, 1938–1942 (2000).
18. Hanks, S.K., Quinn, A.M. & Hunter, T. *Science* **241**, 42–52 (1988).
19. Branger, J. *et al. J. Immunol. In the press* (2002).
20. Cirillo, P.F., Gilmore, T.A., Hickey, E., Regan, J. & Zhang, L.H. *Aromatic Heterocyclic Compounds as Antiinflammatory Agents*. World Patent Application WO-00043384 (2000).
21. Pav, S. *et al. Protein Sci.* **6**, 242–245 (1997).
22. Brünger, A.T. *et al. Acta Crystallogr. D* **54**, 905–921 (1998).
23. Jones, T.A., Zou, J.Y., Cowan, S.W. & Kjeldgaard, M. *Acta Crystallogr. A* **47**, 110–119 (1991).
24. Raingeaud, J., Whitmarsh, A.J., Barrett, T., Derijard, B. & Davis, R.J. *Mol. Cell. Biol.* **16**, 1247–1255 (1996).
25. Han, J. *et al. J. Biol. Chem.* **271**, 2886–2891 (1996).
26. Lozanski, G., Ballou, S.P., & Kushner, I. *J. Rheumatol.* **19**, 921–926 (1992).
27. Carson, M. *J. Mol. Graph.* **5**, 103–106 (1987).
28. Evans, S.V. *J. Mol. Graph.* **11**, 134–138 (1993).
29. Nicholls, A., Sharp, K.A., & Honig, B. *Proteins* **11**, 281–296 (1991).